ELSEVIER

Chemosphere 57 (2004) 1107–1114

CHEMOSPHERE

www.elsevier.com/locate/chemosphere

Oxidation of TNT by photo-Fenton process

Ming-Jer Liou [a], Ming-Chun Lu [b,*], Jong-Nan Chen [a]

[a] *Institute of Environmental Engineering, National Chiao Tung University, Hsinchu 300, Taiwan*
[b] *Department of Environmental Resources Management, Chia Nan University of Pharmacy and Science, Tainan 717, Taiwan*

Received 11 December 2003; received in revised form 16 July 2004; accepted 19 July 2004

Abstract

A series of photo-Fenton reactions have been performed for the degradation of 2,4,6-trinitrotoluene (TNT) in a 4.2-l reactor. The degradation reaction rate of TNT followed a pseudo-first-order behavior; and the rate constants for 2.4 mW cm^{-2} UV only, 2.4 mW cm^{-2} UV/H_2O_2, Fenton, photo-Fenton (2.4 mW cm^{-2}) and photo-Fenton (4.7 mW cm^{-2}) were 0.002 min^{-1}, 0.007 min^{-1}, 0.014 min^{-1}, 0.025 min^{-1} and 0.037 min^{-1}, respectively. Increasing the intensity of UV light, and the concentrations of ferrous ions and hydrogen peroxide promoted the oxidation rate under the experimental conditions in this study. The weighting factor (f), the Fe(II)-promoted efficiency (r) and the promoted-UV light efficiency (p) were calculated to clarify their effects on the TNT oxidation. Moreover, the inhibition effect of hydroxyl radical was also observed in both Fenton and photo-Fenton oxidation when the concentration of Fe(II) were higher than 2.88 mM.

Solid phase micro-extraction was first applied to the separation of the organic byproducts from TNT oxidation. GC/MS was employed to identify the byproducts during the Fenton and photo-Fenton oxidation of TNT. These compounds were clarified as 1,3,5-trinitrobenzene, 1-methyl-2,4-dinitrobenzene 2,5-dinitrobenzoic acid and 1,3-dinitrobenzene. By these byproducts, the mechanisms of the methyl group oxidation, decarboxylation, aromatic ring breakage, and hydrolysis can be recognized and demonstrated. The pathway of TNT oxidation by photo-Fenton process was also proposed in this study.

Keywords: TNT; Fenton; Photo-Fenton; Solid phase micro-extraction

1. Introduction

2,4,6-Trinitrotoluene (TNT) has been widely used as an explosive in military all over the world since 1900s, applied in missiles, bombs and torpedoes. A large amount of strong acidic wastewater is produced during the manufacture of TNT. Besides, residuals of TNT in soil can pollute both the environment and the groundwater system (Li et al., 1998). The United States Department of Defense has identified more than 1000 sites of the explosives contamination. TNT contamination occupies more than 95% of these sites and of 87% exceeded permissible levels of the contaminant in groundwater (Rogers and Bunce, 2001). Since the carcinogenic nature and the potential toxicity, the remediation goals of 17.2 mg TNT kg^{-1} soil has been established by the

* Corresponding author. Tel.: +886 6 266 0489; fax: +886 6 266 3411.
E-mail address: mmclu@mail.chna.edu.tw (M.-C. Lu).

0045-6535/$ - see front matter © 2004 Elsevier Ltd. All rights reserved.
doi:10.1016/j.chemosphere.2004.07.053

United States Environmental Protection Agency for the Nebraska Ordnance Plant site (Li et al., 1998).

Hydrogen peroxide is a widely recognized oxidizing agent ($E_0 = 1.80\,V$ at pH = 0), and its application for treating various inorganic and organic pollutants is well demonstrated (Venkatadri and Peters, 1993). However, hydrogen peroxide alone is not effective for degradation of nitro-aromatic compounds (Li et al., 1998). Advanced oxidation process (AOPs) are regarded as the most effective approaches in treatment of wastewater contaminated with organic pollutants (Alnaizy and Akgerman, 1999). An important oxidation process, namely Fenton process, has been effectively used to degrade nitro-aromatic contaminants (Li et al., 1997). In a Fenton process, ferrous ion reacts with hydrogen peroxide to produce hydroxyl radicals, which combine with organic compounds resulting in oxidation, reduction or combination reaction (Kakarla and Watts, 1997).

Fenton reagent can mineralize the target compounds into small fragments, such as carbon dioxide, nitrate and water. A possible mechanism for decomposition of target organic compound, RH, by Fenton process has been proposed as follows (Utset et al., 2000):

$$Fe^{2+} + H_2O_2 \rightarrow Fe^{3+} + {}^{\bullet}OH + OH^- \quad (1)$$

$$RH + {}^{\bullet}OH \rightarrow {}^{\bullet}R + H_2O \quad (2)$$

$$Fe^{3+} + H_2O_2 \rightarrow Fe^{2+} + {}^{\bullet}HO_2 + H^+ \quad (3)$$

$$H_2O_2 + {}^{\bullet}OH \rightarrow {}^{\bullet}HO_2 + H_2O \quad (4)$$

$$Fe^{3+} + {}^{\bullet}HO_2 \rightarrow Fe^{2+} + O_2 + H^+ \quad (5)$$

The produced $^{\bullet}R$ is further decomposed into small fragments. In the process, $^{\bullet}OH$ is the major oxidant to degrade the target organic compound. It is reported that hydroxyl radical can react rapidly with organic contaminants at a diffusion rate from 10^7 to $10^{10}\,M^{-1}\,s^{-1}$ in water and is a nonspecific oxidant (Kakarla and Watts, 1997).

Photo-Fenton process is carried out by applying ultraviolet (UV) light to a Fenton process. By applying UV light, Fe^{2+} can be regenerated via photo-Fenton reaction as follows:

$$Fe^{3+} + H_2O + h\nu \rightarrow Fe^{2+} + {}^{\bullet}OH + H^+ \quad (6)$$

Reduction of Fe^{3+} to Fe^{2+} is helpful to regenerate radicals in several elementary steps of the reaction mechanism (Utset et al., 2000). Furthermore, a hydrogen peroxide can produce two hydroxyl radicals initiated by UV light, according to Eq. (7).

$$H_2O_2 + h\nu \rightarrow 2\,{}^{\bullet}OH \quad (7)$$

Both two routes facilitate the formation of hydroxyl radicals and will promote the degradation rates of organic compounds. Therefore, Fenton and photo-Fenton processes are both regarded as effective approaches for the degradation of recalcitrant organic pollutants (Bier et al., 1999).

In conventional analyses, sample preparation usually involves in removing and concentrating the analytes of interest through liquid–liquid extraction (LLE), solid extraction, or other techniques (Li et al., 1997). These methods have various drawbacks, including tedious preparation time and extravagant use of organic solvent. Solid phase micro-extraction (SPME) excludes most of these drawbacks (Stack et al., 2000). It is an extraction technique for the explosives and byproducts in aqueous samples, in which analytes are adsorbed directly from the sample solution onto a fused-silica filter that is coated with an appropriate stationary phase. The technique can be used to monitor byproducts of aqueous TNT in photo-Fenton oxidation, and can be used with GC/MS spectrometer system to identify the intermediates during oxidation.

The objective of the present study was to explore the TNT oxidation by the photo-Fenton process in a 4.2-l quartz vessel. For comparison, UV, UV/H_2O_2 and Fenton processes were also conducted as the control experiments. Furthermore, the byproducts were identified by SPME technique and GC/MS analysis. Finally, the pathway of TNT oxidation is proposed.

2. Experimental

2.1. Chemicals

Technical grade TNT was obtained from the Department of Applied Chemistry, Chung Cheng Institute of Technology, National Defense University, ROC. Ferrous sulfate, sodium phosphate (Baker, Phillipsburg, USA) and hydrogen peroxide (Ferak, Berlin, Germany) were used as-received. All chemicals were reagent grade. Aqueous solutions used for oxidation reaction were prepared with deionized (DI) water (Millipore Milli-Q).

2.2. Reactor setup

The batch reactor used in photo-oxidation and Fenton oxidation studies is an insulated quartz vessel (15 cm × 15 cm × 26 cm) with an inside diameter capacity of 4.2-l mounted on a steel frame. A quartz vessel was used to ensure the optimal transparency for UV light source. The reactor was equipped with sample ports, pH meter, agitator, and temperature indicators and controllers. In addition, eight low-pressure mercury lamps (GL-10, Toshiba Inc., Japan) of 10 W were assembled around quartz vessel to provide the irradiation. A heater with a temperature controller was used to maintain constant temperature for a series experiments. UVX-25

Radiometer (UVP Inc., USA) was employed for the determination of UV light intensity.

2.3. Procedure

An aqueous solution of 1.0×10^{-5} M TNT was prepared by stirring an excess amount of TNT in DI water overnight. All reaction solutions were adjusted to pH 3.0 with 0.5 N of nitric acid. Fenton and photo-Fenton processes were initiated by adding hydrogen peroxide and ferrous sulfate into TNT solution. The solution was stirred by an agitator at the rate of 1440 rpm and 28 ± 2 °C. During the oxidation reaction, 2.0 ml aliquots were withdrawn at the selected time intervals. As previously reported (Lu et al., 1999), the Fenton reaction cannot occur at pH > 10. Therefore, the Fenton reaction was quenched instantly by adding 0.5 ml of 0.01 M sodium phosphate aqueous into the withdrawn samples. The TNT concentration was determined by a high performance liquid chromatography (LC 295, Perkin Elmer, USA) with a Supelco LC-18-DB column (25 cm × 4.6 mm × 5 μm), equipped with an UV–VIS detector at a wavelength of 254 nm. The mobile phase was a mixture of methanol and water in the volume ratio of 60:40.

2.4. Byproducts analysis

Prior to GC/MS analysis, the samples were extracted and concentrated by SPME technique (APHA, 2000). A polymer-coated fused silica fiber (Supelco, 65 μm polydimethylsiloxane–divinylbenzene) was put in a 50-ml sample solution at 60 °C. After 60 min, the fiber was moved to the injector of GC/MS (Perkin-Elmer Auto System XL) and then the concentrated samples were desorbed in the loop for 2.5 min. The GC/MS used in this study was Turbo Mass Gold Mass Spectrometer, with the NIST Mass Spectral Search Program. The GC/MS was operated at an electron energy of 70 eV, a source temperature of 200 °C, and a scan speed of 0.2 s per scan from 30 to 400 amu. By selected ion and full ion scanning, selected ion monitoring of scans in mass spectrometer is obtained while simultaneously acquiring data in the full scan mode. A 30-m Rex-5MS fused silica column (0.25 mm ID, 0.25 μm film thickness, Restek, USA) was held at 100 °C for 3 min and then heating rate was programmed at 20 °C min^{-1} to 280 °C.

3. Results and discussion

3.1. The factors on the oxidation of TNT

In this study, a 4.2-l quartz vessel was used to explore the oxidation of TNT by photo-Fenton process. Since the energy of UV light was about 470–300 kJ mol^{-1} within the range of the bond energy for most organic compounds (500–250 kJ mol^{-1}), it can excite the electrons of the organic compounds from ground state to excited state, resulting in photo-chemical reaction. Moreover, Fe^{2+} can be simultaneously regenerated through UV light reduction from Fe^{3+} in photo-Fenton reaction to produce more reactive hydroxyl radicals. As a result, Fe^{3+} is not the predominant species at pH 3.

The UV, UV/H_2O_2 and Fenton processes were carried out as the control experiments for the comparison of TNT oxidation with different processes. Organic compounds can be decomposed under the exposure to UV light. However, the photochemical degradation of TNT with 2.4 mW cm^{-2} UV only was quite weak. Fig. 1 shows the residual ratio of TNT after 120 min degradation for 2.4 mW cm^{-2} UV only, 2.4 mW cm^{-2} UV/H_2O_2, Fenton, photo-Fenton (2.4 mW cm^{-2} UV) and photo-Fenton (4.7 mW cm^{-2} UV) processes. By applying pseudo-first-order reaction model, the rate constants and half-lives of the five processes were also obtained and listed in Table 1. Results also show that the oxidation rates of TNT followed the sequence: 2.4 mW cm^{-2} UV

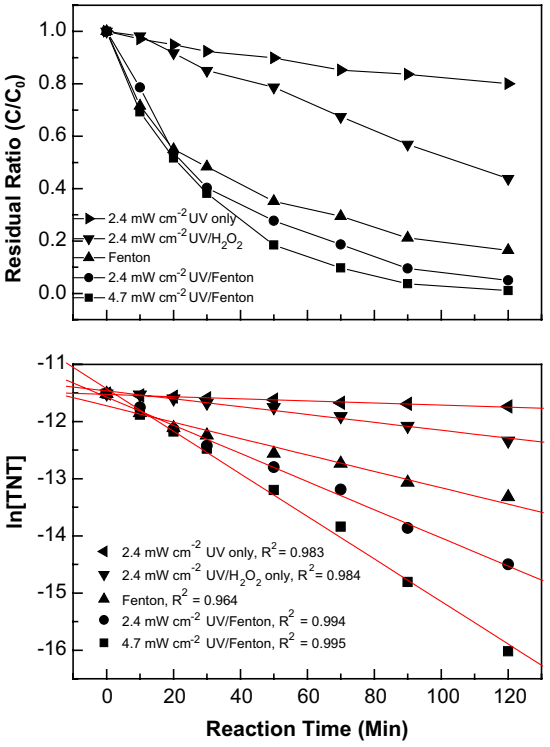

Fig. 1. Comparison of UV process (▶), UV/H_2O_2 process (▼), Fenton process (▲), photo-Fenton process with 2.4 mW cm^{-2} UV (●), and photo-Fenton process with 4.7 mW cm^{-2} UV (■) processes in oxidizing TNT. Experimental conditions: [TNT] = 1.0×10^{-5} M, [H_2O_2] = 0.29 M, [Fe(II)] = 7.2×10^{-4} M, pH = 3.0, temperature = 28 ± 2 °C.

Table 1
Pseudo-first-order constants for photo-oxidation and Fenton oxidation TNT

	Advanced oxidation processes				
	2.4 mW cm^{-2} UV	2.4 mW cm^{-2} UV/H_2O_2	Fenton	Photo-Fenton (2.4 mW cm^{-2} UV)	Photo-Fenton (4.7 mW cm^{-2} UV)
Residual ratio after 120 min (%)	83.4	43.8	16.4	5.0	1.1
Decomposing rate constant (k, min^{-1})	0.002	0.007	0.014	0.025	0.037
Decomposition half-life ($t_{1/2}$, min)	376.7	100.8	48.4	28.1	18.6

Experimental conditions: [TNT] = 1.0×10^{-5} M, [Fe^{2+}] = 0.72 mM, [H_2O_2] = 0.29 M, pH = 3.0 and temperature = 28 ± 2 °C.

only < 2.4 mW cm^{-2} UV/H_2O_2 < Fenton < photo-Fenton (2.4 mW cm^{-2} UV) < photo-Fenton (4.7 mW cm^{-2} UV).

Table 1 also shows that either introducing UV light or increasing the UV intensity accelerated the rate of Fenton oxidation for 0.01 mM of TNT. This is because UV-light can both induce the photolysis of hydrogen peroxide and regenerate ferrous ions to produce hydroxyl radicals (Li et al., 1997). Similar phenomenon also happened by adding hydrogen peroxide and ferrous ions into the reaction mixture. Hence, a series of weighting factors for 0.29 M hydrogen peroxide ($f_{H_2O_2}$), 0.72 mM ferrous ions ($f_{Fe^{2+}}$) and UV light ($f_{2.4\,mW\,cm^{-2}}$, $f_{4.7\,mW\,cm^{-2}}$) were first quantitatively extracted from our investigation in quartz-pilot system. Therefore, $f_{H_2O_2}$ is defined as follows:

$$f_{H_2O_2} \times t_{1/2\ \text{with}\ H_2O_2} = t_{1/2\ \text{without}\ H_2O_2} \quad (8)$$

$t_{1/2\,\text{with}\,H_2O_2}$ is the half-life of photo-oxidation process with H_2O_2 addition, and $t_{1/2\ \text{without}\ H_2O_2}$ is that without H_2O_2. By comparing the half-lives with UV and UV/H_2O_2 processes, as listed in Table 1, $f_{H_2O_2}$ is obtained as 3.74. By similar definition and operations of the weighting factors, $f_{Fe^{2+}}$, $f_{4.7\,mW\,cm^{-2}}$ and $f_{2.4\,mW\,cm^{-2}}$ can be obtained as 3.58, 2.60 and 1.72, respectively.

Because 0.29 M of H_2O_2 played an important role of the precursor of OH radical in a series of oxidation, addition of hydrogen peroxide seemed to be the most effective way to accelerate the oxidation of TNT. Without considering the effect of [Fe^{2+}], other weighting factors followed the sequence: $f_{Fe^{2+}}$ (3.58; 0.72 mM ferrous ions) > $f_{4.7\,mW\,cm^{-2}}$ (2.60; 4.7 mW cm^{-2}) > $f_{2.4\,mW\,cm^{-2}}$ (1.72; 2.4 mW cm^{-2}). Of the most importance, weighting factors are profitable to predict the half-life of TNT oxidation in different processes.

3.2. Effect of [Fe^{2+}] and UV light on the oxidation of TNT

Three concentrations of Fe^{2+} (1.44 mM, 2.88 mM and 4.32 mM) were applied to study its effect on the TNT oxidation. Fenton and photo-Fenton processes were carried out for comparison. It is observed that the degradation efficiency was promoted with either increasing Fe(II) concentration or by using a 2.4 mW cm^{-2} UV light. Fig. 2 shows that the concentrations of ferrous ions affected the efficiency of TNT destruction obviously. The residual ratio of TNT after 120 min decreased as the concentration of Fe(II) used in the Fenton process increased. In addition, the introduction of UV light promotes the degradation of TNT further. By the pseudo-first-order model, the rate constants from Fenton and photo-Fenton reactions can be obtained and listed in Table 2.

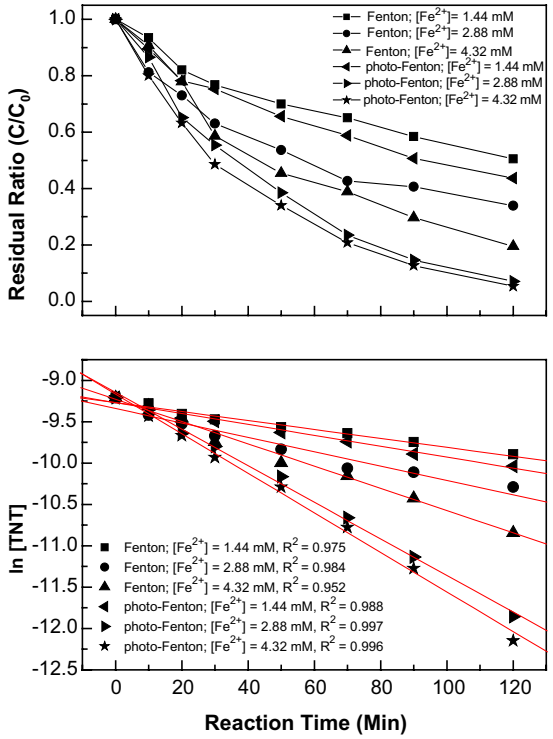

Fig. 2. Effects of [Fe^{2+}] on the photo-Fenton oxidation of TNT. Experimental conditions: [TNT] = 1.1×10^{-4} M, [H_2O_2] = 0.29 M, pH = 3.0, temperature = 25 °C; [Fe(II)] = 1.44×10^{-3} M (■), [Fe(II)] = 1.44×10^{-3} M and 2.4 mW cm^{-2} UV (◀), [Fe(II)] = 2.88×10^{-3} M (●), [Fe(II)] = 4.32×10^{-3} M (▲), [Fe(II)] = 2.88×10^{-3} M and 2.4 mW cm^{-2} UV (▶), [Fe(II)] = 4.32×10^{-3} M and 2.4 mW cm^{-2} UV (★).

Table 2
Pseudo-first-order constants for UV-promoted efficiency (p) and Fenton oxidation of TNT

Fe(II) (mM)	Fenton k_F (min^{-1})	Photo-Fenton (2.4 mW cm^{-2} UV) k_P (min^{-1})	UV-promoted efficiency ($p = k_P/k_F$)
1.44	0.0055	0.0067	1.22
2.88	0.0087	0.0220	2.52
4.32	0.0136	0.0240	1.76

Experimental conditions: [TNT] = 1.1×10^{-4} M, [H_2O_2] = 0.29 M, pH = 3.0 and temperature = 25 °C.

Results show obviously that increasing concentration of Fe(II) resulted in increasing the degradation rate constant directly. The enhancement due to increasing [Fe^{2+}] was called the Fe(II)-promoted efficiency (r) and defined as the promoted coefficient of rate constant ($k_{\text{high Fe(II)}}/k_{1.44\text{ mM Fe(II)}}$) at higher concentration normalized with the least rate constant at 1.44 mM Fe(II). The catalytic efficiency of Fe(II) shown in Table 2 reveals that the Fe(II) efficiency at higher concentration of Fe(II) was larger than that at lower concentration of Fe(II). In addition, the Fe(II) efficiency of photo-Fenton process with 2.4 mW cm^{-2} UV light was larger than that of Fenton process at the same concentration of Fe(II). Similar results have been reported by Li et al. (1997) that Fenton oxidation under the UV light condition would accelerate mineralization, faster than the efficiency under the dark condition. Li et al. (1998) also reported that photo-Fenton process exhibited good decomposition ability on explosives such as TNT, DNT and MNT because Fe^{2+} can be regenerated through photo-reduction of Fe^{3+} to produce highly reactive hydroxyl radicals. In this study, the photo-Fenton (2.4 mW cm^{-2}) process at 4.32 mM of Fe(II) was proven to have the highest decomposition efficiency ($k = 0.024\ min^{-1}$). It means that photo-reduction of Fe(III) (Eq. (6)) dominates the photo-Fenton oxidation. However, when the concentration of Fe(II) was adjusted to 4.32 mM, the Fe(II)-promoted efficiency of photo-Fenton oxidation slowed down. It is due to the ·OH inhibition effect, which will be further discussed in detail later.

In Table 2, k_F is defined as the rate constant of Fenton oxidation, and k_P is defined as the rate constant of the photo-Fenton oxidation. When k_P is larger than k_F, the UV-promoted efficiency ($p = k_P/k_F$) is greater than one. Results show that the photo-Fenton oxidation was more effective than the Fenton oxidation. It also indicates that the ·OH inhibition effect could occur at higher Fe(II) concentration for photo-Fenton oxidation. In fact, there are many probable mechanisms in present inhibition. Kavitha and Palanivelu (2004) reported that carboxylic acids were formed as end products during the photo-Fenton oxidation of phenol. Safarzadeh-Amiri and Bolton (1997) also reported that Fe(II) could be regenerated in photo-decarboxylation of ferric carboxylates as shown in Eq. (9), and Fe(II) also generated by aquahydroxocomplexes of Fe(III) strongly absorb UV light (Faust and Hoigne, 1990) as shown in Eq. (10). Therefore, Fe(II) was regenerated continuously by the UV light-induced reduction reaction in photo-Fenton oxidation. Increasing the concentration of Fe(II) will lead to an increase of Fe(III) complex compounds. The reason is the rate of degradation could be limited by the reduction of the photonic flux in this reaction system. Furthermore, H_2O_2 is also the predominant ·OH scavenger because the concentration of H_2O_2 is very high as shown in Eq. (4) and Fe(II) could be regenerated as shown in Eq. (5).

$$Fe^{3+}(RCO_2)^{2+} + h\nu \rightarrow Fe^{2+} + CO_2 + R^{\bullet} \quad (9)$$

$$Fe^{3+}OH^{2+} + h\nu \rightarrow Fe^{2+} + {}^{\bullet}OH \quad (10)$$

In addition, the ·OH can be generated from both photolysis of H_2O_2 and photo-reduction of Fe(III). However, the excess amount of ·OH generated from the photolysis of H_2O_2 will inhibit the ·OH generated from the Fenton reaction due to higher Fe(II) concentration. The phenomenon has been estimated in our study that seven explosives were degraded by photo-Fenton oxidation previously (Liou et al., 2003). Therefore, the UV-promoted efficiency (k_P/k_F) on Fenton oxidation in this study will decrease as the Fe(II) concentration beyond the threshold value (2.88 mM in this study).

3.3. Byproducts of TNT oxidation by photo-Fenton oxidation

Previous researchers often reported on the byproducts of Fenton oxidation of explosives by using LLE, and analyzed by LC/MS or GC/MS (Li et al., 1997; Zoh and Stenstrom, 2002). In order to verify accurately the presence of the organic intermediate byproducts from photo-Fenton oxidation, the reaction byproducts of TNT were extracted by using SPME, and then analyzed by using GC/MS. Stack et al. (2000) had applied SPME technique to determine four common trihalomethanes (THMs) in potable and recreational water. There are four byproducts identified from the decomposed products by SPME/GC/MS integrated system in this study.

The samples containing byproducts were obtained at various times during the oxidation of 1.0×10^{-4} M TNT by photo-Fenton process with 2.4 mW cm^{-2} UV lights. Fig. 3a shows the mass chromatograms (Retention time,

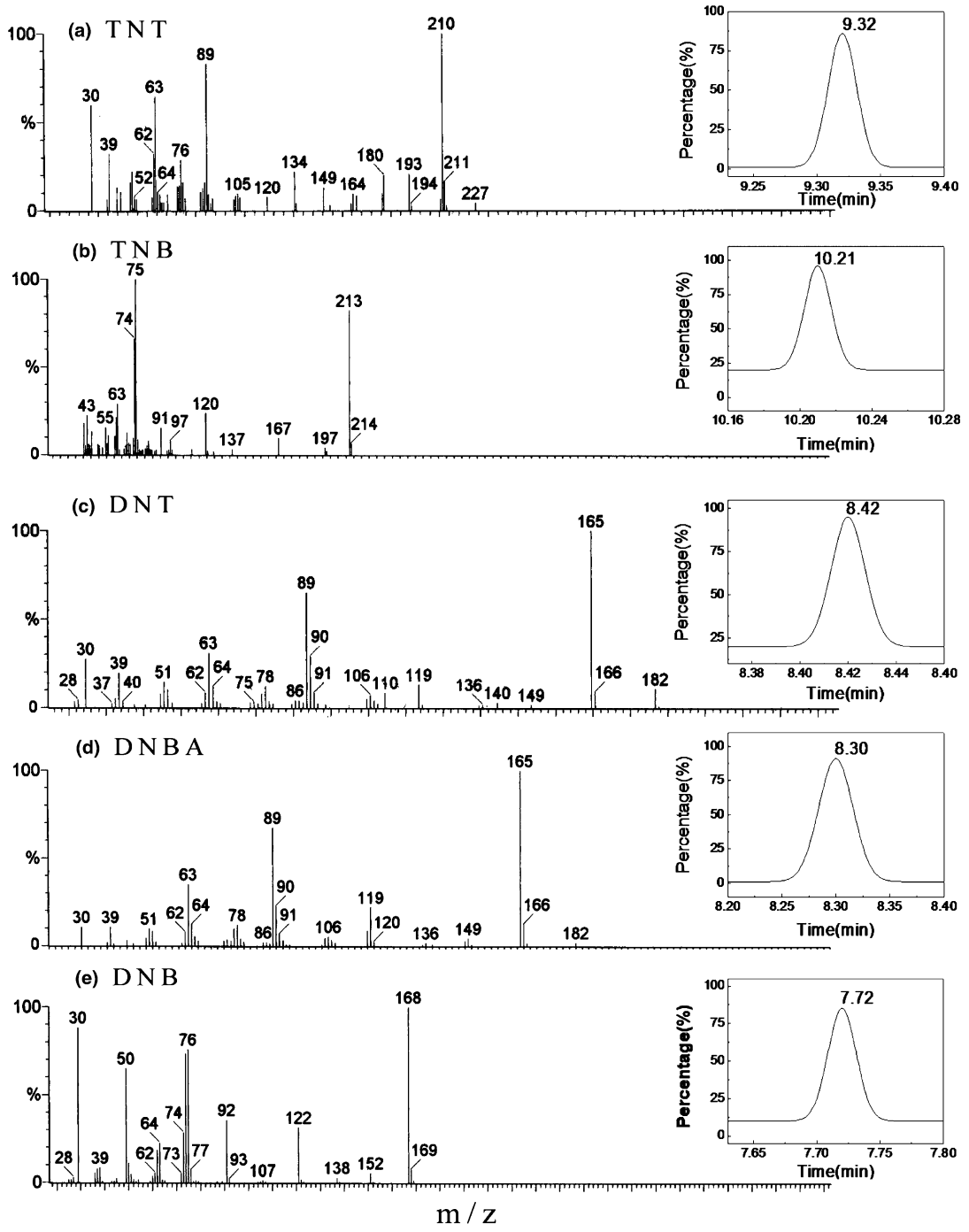

Fig. 3. The GC/MS spectra of byproducts in photo-Fenton oxidation of TNT. Experimental conditions: [TNT] = 1.1×10^{-4} M, pH = 3.0, temperature = 25 °C, 2.4 mW cm^{-2} UV, [H_2O_2] = 0.29 M and [Fe(II)] = 7.2×10^{-4} M.

Rt = 9.32 min) and mass spectrum of TNT at $t = 0$ in photo-Fenton oxidation. A main base peak at $m/z = 210$ was found in the typical EI mass spectrum, corresponding to loss of 17 (the mass of OH). Among the samples of photo-Fenton process, many important spectra were found to prove the degradation mechanism of TNT. After 10 min of photo-Fenton reaction, a byproduct peak was detected (Rt = 10.21 min) and its mass spectrum is confirmed to 1,3,5-trinitrobenzene (TNB), shown as Fig. 3b. The highest mass peak is 75

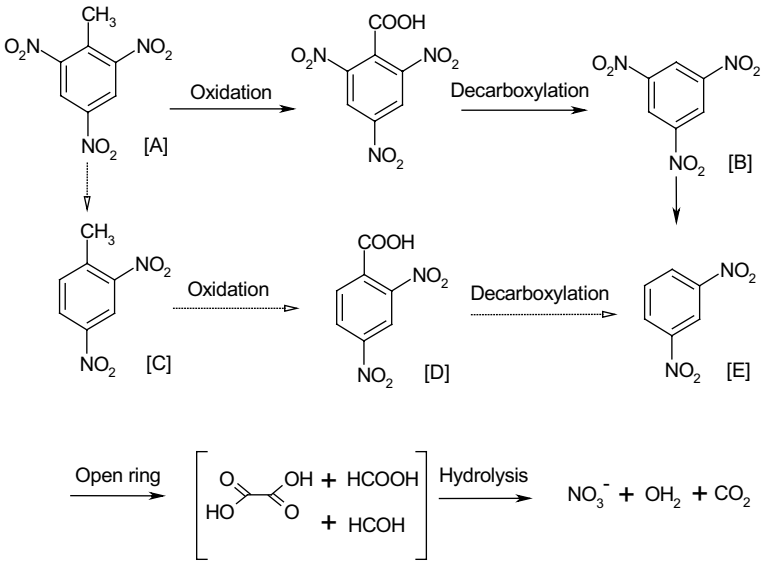

Fig. 4. The proposed mechanism for the decomposition of TNT in photo-Fenton process.

(benzene group, C_6H_3), corresponding to loss of 138 (three functional groups, $3NO_2$).

The signal of TNB on GC increased gradually as the oxidation time increased, revealing that TNB is the predominant byproduct in photo-Fenton process. The second byproduct (C) shown in Fig. 3c was 2,4-dinitrotoluene (DNT). The DNT is also a precursor during the synthesis of TNT and the DNT signal on GC spectrum decreases gradually as the oxidation time increases. At Rt = 8.42 min and base peak $m/z = 165$ ($C_6H_3(NO_2)_2$) was detected, corresponding to further loss of 17 (methyl group, CH_3) from DNT.

Fig. 3d (byproduct (D), Rt = 8.3 min, base peak $m/z = 165$) and Fig. 3e (byproduct (E), Rt = 7.72 min, base peak $m/z = 76$) present very important evidences for the intermediates hypothesis. According the GC/MS spectra, they could be proven as 2,5-dinitro-benzoic acid (DNBA) and 1,3-dinitrobenzene (DNB), respectively. In fact, byproducts C, D and E show that the first step in photo-Fenton oxidation of TNT was likely the oxidation of methyl group and then decarboxylation occurred.

Concerning the degradation mechanism of TNT, there are three steps generally expected, including methyl group oxidation, decarboxylation of aromatic acid (Urbanski, 1964) and mineralization of nitro groups (March, 1985). Li et al. (1997) had reported the intermediates of Fenton oxidation of TNT were 2,4,6-trinitrobenzonic acid and TNB by using LC/MS. According to these evidences, it indicates that the initial TNT destruction could be occurred after the methyl group oxidation and then the decarboxylation of 2,4,6-trinitrobenzoic acid. This is because that the $-CH_3$ groups have electron-releasing abilities, leading to increase the reactivity of TNT. They also observed the $-NO_2$ groups of TNT were stoichiometrically removed and oxalate was produced simultaneously. In other words, the $-NO_2$ group, an electron-withdrawing group, reduced the reactivity of TNT.

Tanaka et al. (1997) reported that organic acids and nitrates were the final products of the cleavage of aromatic rings. Among the organic acids detected, formic and oxalic acids have the highest value in concentrations. This step involved the cleavage of aromatic ring and hydrolysis. Since both reactions can occur, but which one is prior to another has not been reported for the absence of the captured intermediates. These byproducts could be degraded gradually into final products of organic acids, water and carbon dioxide (Zoh and Stenstrom, 2002). Therefore, the degradation mechanism of photo-Fenton of TNT can be proposed as shown in Fig. 4.

4. Conclusion

The factors affecting the rate constants in the photo-oxidation of TNT were discussed and quantified in this study. The oxidation rates of TNT follow the sequence: UV only < UV/H_2O_2 < Fenton < photo-Fenton. Three parameters, namely light intensity, hydrogen peroxide and ferrous ion, were employed to explore their effect on the efficiency of TNT oxidation. The weighting factor (f) of each introduction follows the ranking as $f_{2.4\,mW\,cm^{-2}}$ (1.72) < $f_{4.7\,mW\,cm^{-2}}$ (2.60) < $f_{Fe^{2+}}$ (3.58) < $f_{H_2O_2}$ (3.74) at 1.0×10^{-5} M TNT.

Increasing concentrations of Fe(II) and introducing UV light promoted the decomposing rate in photo-Fenton reaction. However, both the Fe(II)-promoted efficiency and the UV-promoted efficiency were reduced when the concentration of Fe(II) was higher than 2.88 mM. Five byproducts were separately identified as TNB, DNT, DNBA, and DNB by GC/MS. The degradation mechanism is proposed by identifying the products for each step with SPME/GC/MS technique. The prior step in mineralization is the open-ring reaction, and then the hydrolysis of $-NO_2$ groups occurs.

References

Alnaizy, R., Akgerman, A., 1999. Oxidative treatment of high explosives contaminated wastewater. Water Res. 33 (9), 2021–2030.

APHA, AWWA, and WPCF, 2000. Supplement to Standard Methods for the Examination of Water and Wastewater, 20th ed. Method 6040D. Solid-Phase Microextraction (SPME), APHA, Denver, Colorado, USA.

Bier, E.L., Singh, J., Li, Z.M., Comfort, S.D., Shea, P.J., 1999. Remediating hexahydro-1,3,5-trinitro-1,2,5-triazine-contaminated water and soil by Fenton oxidation. Environ. Toxicol. Chem. 18, 1078–1084.

Faust, B.C., Hoigne, J., 1990. Photolysis of Fe(III)-hydroxy complexes as sources of OH radicals in clouds, fog and rain. Atmos. Environ. 24A, 79–89.

Kakarla, P.K.C., Watts, R.J., 1997. Depth of Fenton-like oxidation in remediation of surface soil. J. Environ. Eng. 123, 11–17.

Kavitha, V., Palanivelu, K., 2004. The role of ferrous ion in Fenton and photo-Fenton processes for the degradation of phenol. Chemosphere 55, 1235–1243.

Li, Z.M., Comfort, S.D., Shea, P.J., 1997. Destruction of 2,4,6-trinitrotoluene by Fenton oxidation. J. Environ. Qual. 26, 480–487.

Li, Z.M., Shea, P.J., Comfort, S.D., 1998. Nitrotoluene destruction by UV-catalyzed Fenton oxidation. Chemosphere 36, 1849–1865.

Liou, M.J., Lu, M.C., Chen, J.N., 2003. Oxidation of explosives by Fenton and photo-Fenton processes. Water Res. 37, 3172–3179.

Lu, M.C., Chen, J.N., Chang, C.P., 1999. Oxidation of dichlorvos with hydrogen peroxide using ferrous ion as catalyst. J. Hazard. Mater. B65, 277–288.

March, J., 1985. Advance Organic Chemistry, third ed. Wiley, Canada, p. 786.

Rogers, J.D., Bunce, N.J., 2001. Review paper treatment methods for the remediation of nitro aromatic explosives. Water Res. 35, 2101–2111.

Safarzadeh-Amiri, A., Bolton, J.R., 1997. Ferrioxalate-mediated photodegradation of organic pollutants in contaminated water. Water Res. 31, 787–798.

Stack, M.A., Fitzgerald, G., O'Connell, S., James, K.J., 2000. Measurement of trihalomethanes in potable and recreational waters using solid phase micro extraction with gas chromatography–mass spectrometry. Chemosphere 41, 1821–1826.

Tanaka, K., Luesaiwong, W., Hisanaga, T., 1997. Photocatalytic degration of mono-, di- and trinitrophenol in aqueous TiO_2 suspension. J. Mol. Catal. A 122, 67–74.

Urbanski, T., 1964. Chemistry and Technology of Explosives, vol. 1. Pergamon Press, New York, pp. 291–295.

Utset, B., Garcia, J., Casado, J., Doménech, X., Peral, J., 2000. Replacement of H_2O_2 by O_2 in Fenton and photo-Fenton reactions. Chemosphere 41, 1187–1192.

Venkatadri, R., Peters, R.W., 1993. Chemical oxidation techniques: UV/H_2O_2, Fenton reagent, and titanium dioxide-assisted photocatalysis. Hazard. Waste Hazard. 10, 107–149.

Zoh, K.D., Stenstrom, M.K., 2002. Fenton oxidation of hexahydro-1, 3, 5-trinitro-1, 3, 5-triazine (RDX) and octahydro-1, 3, 5, 7-tetranitro-1, 3, 5, 7-tetrazocine (HMX). Water Res. 36, 1331–1341.